

Optimization of Ti/Ta₂O₅–SnO₂ electrodes and reaction parameters for electrocatalytic oxidation of methylene blue

Shestakova, M., Graves, J., Sitarz, M. & Sillanpää, M.

Author post-print (accepted) deposited by Coventry University's Repository

Original citation & hyperlink:

Shestakova, M, Graves, J, Sitarz, M & Sillanpää, M 2016, 'Optimization of Ti/Ta₂O₅–SnO₂ electrodes and reaction parameters for electrocatalytic oxidation of methylene blue' *Journal of Applied Electrochemistry*, vol. 46, no. 3, pp. 349-358.

<https://dx.doi.org/10.1007/s10800-016-0925-5>

DOI 10.1007/s10800-016-0925-5

ISSN 0021-891X

ESSN 1572-8838

Publisher: Springer

The final publication is available at Springer via <http://dx.doi.org/10.1007/s10800-016-0925-5>

Copyright © and Moral Rights are retained by the author(s) and/ or other copyright owners. A copy can be downloaded for personal non-commercial research or study, without prior permission or charge. This item cannot be reproduced or quoted extensively from without first obtaining permission in writing from the copyright holder(s). The content must not be changed in any way or sold commercially in any format or medium without the formal permission of the copyright holders.

This document is the author's post-print version, incorporating any revisions agreed during the peer-review process. Some differences between the published version and this version may remain and you are advised to consult the published version if you wish to cite from it.

1 **Optimization of Ti/Ta₂O₅-SnO₂ electrodes and reaction parameters for electrocatalytic oxidation of**
2 **methylene blue**

3 *Marina Shestakova^{a*}, John Graves^b, Maciek Sitarz^c, Mika Sillanpää^a*

4 ^a *Laboratory of Green Chemistry, Faculty of Technology, Lappeenranta University of Technology, Sammonkatu 12,*
5 *FI-50130 Mikkeli, Finland*

6 ^b *Functional Materials Applied Research Group, Coventry University, Priory Street, Coventry, CV1 5FB, United*
7 *Kingdom.*

8 ^c *AGH University of Science and Technology, Faculty of Materials Science and Ceramics, Av. Mickiewicza 30, 30-*
9 *059 Cracow, Poland.*

10 *Corresponding author. Tel.: +358 50 594 8015. E-mail address: marina.shestakova@hotmail.com (M. Shestakova).

11 **Abstract**

12 Among existing water treatment methods for organic containing wastewaters advanced oxidation processes (AOP)
13 and particularly electrocatalytic oxidation is a technique allowing to reach high degradation and mineralization
14 efficiencies. Electrodes tested for use in electrocatalytic oxidation processes contain either expensive or
15 platinum/group metals such as Pt, Ru, Ir, Pd or boron doped diamond (BDD) and Sb and Pb compounds which are
16 toxic for the environment. Thereby, there is a need for environmentally friendly and less expensive electrodes. The
17 objectives of this research were to optimize annealing temperature of Ti/Ta₂O₅-SnO₂ electrodes, establish the
18 working media for organic compound oxidation processes as well as check degradation, mineralization and current
19 efficiencies for methylene blue (MB) dye oxidation. Decolourisation efficiency of 95% was achieved in 2h at pH =
20 6.5. Neutral media showed also higher efficiency towards COD decrease which was equal to 85% after 2 h of
21 electrolysis. The lowest energy consumption of 7.7 kWh m⁻³ required for 100% decolourisation was observed for the
22 electrodes annealed at 550 °C at pH = 2. The highest current efficiency (CE) of 10.1% attributed to 80% of COD
23 reduction was obtained for the electrode annealed at 550 °C at pH = 6.5. The optimization data allow further
24 extrapolating of electrocatalytic oxidation process on Ti/Ta₂O₅-SnO₂ electrodes to pilot scale.

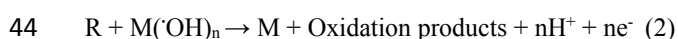
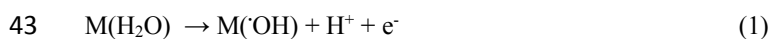
25 **Keywords.** Electrocatalysis, Electrolysis, Ti/Ta₂O₅-SnO₂ electrodes, Methylene Blue

26 **1 Introduction**

27 Water, energy, food and climate securities are the main global challenges nowadays where water is the core of the
28 water-food-energy-climate nexus [1]. Spent industrial and domestic water cannot be directly released back to the
29 environment or returned to a technological cycle since it is contaminated with mechanical impurities, organic and
30 inorganic pollutants.

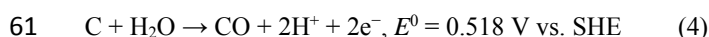
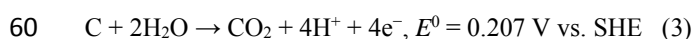
31 Traditional treatment methods of wastewater containing organic compounds are biological treatment, chemical
32 oxidation, coagulation and adsorption. However, these methods are inefficient towards persistent organic
33 compounds such as insecticides, pesticides, pharmaceuticals etc. [2] In addition, a significant group of pollutants
34 such as dyes which are widely used in textile, tannery, pulp and paper and pharmaceutical industries were found
35 resistant to microorganism attack and cannot be efficiently treated by biological methods [3]. Despite the ease of
36 implementation, all traditional wastewater treatment methods have the main disadvantage of the secondary waste
37 formation. Spent adsorbents, coagulation, sedimentation and sewage sludge should be regenerated or disposed
38 which requires additional costs and working areas.

39 Advanced oxidation processes (AOP) and particularly electrocatalytic oxidation are promising techniques allowing a
40 complete mineralization of resistant organic pollutants to simple molecules like CO₂ and H₂O without generation of
41 secondary wastes. Electrocatalytic oxidation of organic pollutants by direct electrolysis occurs by means of
42 interaction of adsorbed hydroxyl radicals on the electrode surface (M) with an organic pollutant (R) [4-5]:



45 Moreover, along with high mineralization efficiencies achieved by anodic oxidation, electrocatalytic methods are
46 easy to implement and automate. The most commonly used electrodes for electrocatalytic oxidation of organic
47 compounds are BDD, Pt, Sb-doped RuO₂/TiO₂, Ti/IrO₂-SnO₂-Sb₂O₅, Ti-Pt/β-PbO₂, Ti/Sb-SnO₂, Ti/PbO₂,
48 Ti/(IrO₂+Ta₂O₅), Ti/SnO₂-Sb₂O₅, Ti/SnO₂-Sb₂O₅-PtO_x, Ti/SnO₂-Sb₂O₅-RuO₂, Ti/RuO₂-IrO₂ [6-15]. As it can be
49 seen all of them contain either expensive compounds like diamond, Pt, Ru, Ir or potentially environmentally toxic
50 compounds such as Pb and Sb. Therefore there is a search for less expensive, less toxic electrodes with a high
51 electrocatalytic oxidation efficiency. Over the last few years phosphotungstic acid/neutral red intercalated
52 montmorillonite composite (PTA/NR-MMT) film electrodes assembled on a graphite electrode, magnetite/reduced
53 graphene oxide (Fe₃O₄/RGO) composite electrodes, Ni-doped nanoporous carbon electrodes, lithium-doped Ta₂O₅

54 film coated electrodes etc. were found active towards oxidation of N-acetylcysteine, methyl jasmonate, propargyl
55 alcohol, ascorbic acid and glucose [16-20]. However, the above mentioned electrodes have been only
56 electrochemically and physically characterized and so far, there is no information on electrolysis experiments,
57 degradation efficiencies, COD and TOC decrease of organic pollutants using these types of electrodes. Moreover,
58 carbon-containing electrodes are expected to be suitable for detection of organic compounds rather than for their
59 oxidation in wastewaters due to low potential for carbon corrosion [21] which is shown in the following reactions:



62 Recently novel Ti/Ta₂O₅-SnO₂ electrodes were found potentially active towards electrocatalytic oxidation of organic
63 compounds and particularly methylene blue (MB) dye [22]. However, the best process conditions for electrode
64 preparation and electrocatalytic oxidation of MB still have to be determined. In this paper, we report for the first
65 time on the optimization of the annealing temperature of Ti/Ta₂O₅-SnO₂ electrodes and determine the best media
66 conditions for electrolysis processes in terms of energy and mineralization efficiency.

67 **2 Experimental**

68 *2.1 Electrode preparation*

69 Ti/Ta₂O₅-SnO₂ electrodes with the nominal composition of Ta(x) - Sn (100 - x) where x = 7.5 at.% were prepared
70 by a thermal decomposition and drop casting technique of the precursor solution onto a titanium substrate [23]. The
71 detailed preparation method is described elsewhere [22]. The total concentration of metals ions was equal to 0.04
72 M. The total number of active Ta₂O₅-SnO₂ layers forming the ultrathin film deposited on the titanium substrate was
73 eight. Three different annealing temperatures of 450, 550 and 650 °C were used for the electrode preparation. After
74 10 h final air-annealing, without additional air circulation in muffle furnace, the electrodes were cooled down and
75 washed for 10 min in an ultrasonic bath and finally dried at 105 °C. Electrodes were weighed after etching and at the
76 final stage of preparation. Ta₂O₅-SnO₂ material deposition was equal to 1.1 mg cm⁻² ± 3%.

77 All chemicals used for electrodes and working solution preparation were of analytical grade and used without
78 further purification. Tantalum (V) chloride (99.99% trace metal basis, Sigma-Aldrich), tin (II) chloride dehydrate
79 (≥99.99% trace metals basis, Sigma-Aldrich) and absolute ethanol (Baker Analyzed' VLSI grade, J.T. Baker) were

80 used for the precursor solution preparation. Titanium substrate pretreatment was conducted in 10 wt.% NaOH
81 ($\geq 98\%$ anhydrous, Sigma-Aldrich) and 18 wt. % boiled hydrochloric acid (pro analysis, Fluka).

82 *2.2 Physicochemical and electrochemical characterization of the electrodes*

83 All electrodes were physically and electrochemically characterized. Microstructure of the produced materials was
84 examined by means of scanning electron microscope (SEM) (Hitachi S-4800, Japan) with an attachment for
85 chemical analysis of specimen in microareas with energy dispersive x-ray spectroscopy (Ametek, S4800, USA). X-
86 ray diffraction (XRD) measurements at small incident angle (GID) were performed using the Empyrean
87 (Panalytical) diffractometer with Cu anode and the focusing mirror. The range of measurement was from 20° to 80°
88 of the angle 2θ , with constant omega angle = 1. The measurement step was 0.02° , with measurement time of 2.4 s
89 per step.

90 The electrochemical characterization of the electrodes was conducted with an Autolab PGSTAT12
91 Galvanostat/Potentiostat using cyclic voltammetry (CV) measurements in a conventional three electrode cell (200
92 ml. The potentiostat was computer-controlled by GPES EcoChimie software. The prepared Ti/Ta₂O₅-SnO₂
93 electrodes, with a surface area of 2.2 cm² controlled with Teflon ribbon, were used as working electrodes. Gold disc
94 electrode of 2 mm diameter (Metrohm-Autolab) was used as a working electrode for comparison experiment. A
95 coiled platinum wire served as a counter electrode and saturated calomel electrode (SCE) was used as a reference
96 electrode. All CV measurements were performed versus this reference electrode between 0.15 and 2 V potential
97 limits at a scan rate of 50 mV s⁻¹. Electrode conditioning, at potentials of 0.2 V for 15 s and 1.2 V for 5 s, was
98 applied before each measurement as a pretreatment step. CV measurements were conducted in supporting electrolyte
99 solution of 0.1 M Na₂SO₄ (anhydrous ACS reagent, Sigma-Aldrich), aqueous solution of 0.1 M Na₂SO₄ and 0.1 mM
100 MB (Certistain, Merck) at room temperature in acidic (pH = 2), basic (pH = 12) and neutral (pH = 6.5) media. pH
101 was adjusted by H₂SO₄ and NaOH. An aqueous solution of 0.5 mM potassium hexacyanoferrate (II) trihydrate (99%
102 trace metal basis, Riedel-de-Haën) and 0.1 M Na₂SO₄ was used for CV measurements to estimate the active surface.
103 The supporting electrolyte solution and aqueous solution of Na₂SO₄ and MB are hereafter referred to as the blank
104 and working solution respectively. Ultrapure water (18.2 MΩ cm) was used for the solution preparation and
105 deoxygenated by bubbling nitrogen before every CV measurement. Hielscher UP-50H ultrasonic probe (Sonotrode

106 MS3, 50 W maximum output power) with 80% amplitude was used for conducting CV measurements in the
107 ultrasonic field.

108 2.3 Electrolysis and degradation efficiency control

109 Electrochemical oxidation experiments were carried out in a jacketed reactor placed on a magnetic stirrer. The
110 stirring rate was 1000 rpm. A constant temperature of 25 ± 2 °C was maintained by water circulation through a
111 jacketed cooler. 30 ml samples of working solution were used for degradation experiments. The Ti/Ta₂O₅-SnO₂
112 electrodes with a surface area of 2.2 cm² were used as anodes and Ti plate of the same surface area served as the
113 cathode. The distance between electrodes was 1 cm. Electrolyses at a constant current of 20 mA (current density of 9
114 mA cm⁻²) were carried out using a GW Instek PSM-6003 power supply.

115 The decolourisation of MB was monitored by UV-Vis spectrophotometer (Lambda 45, Perkin Elmer) by measuring
116 the absorbance of light by MB at 664 nm in neutral and acidic media and at 591 nm in basic media. Chemical
117 Oxygen Demand (COD) was determined by means of a Hach Lange DRB 200 system. The non-purgeable organic
118 carbon (NPOC) content was measured with a TOC analyzer (TOC-Vcpn, Shimadzu, Japan).

119 The energy consumption (EC) per volume of treated working solution (kWh m⁻³) and current efficiency (CE, %) of
120 electrolysis processes in different media were calculated according to the following equations [24]:

$$121 \quad EC \text{ (kWh m}^{-3}\text{)} = IVt/V_s \quad (1)$$

$$122 \quad CE \text{ (\%)} = ((\Delta COD)FV_s/8It) \times 100 \quad (2)$$

123 where I is the average applied current (A), V is the average cell voltage (V), t is the electrolysis time (h in the case of
124 EC) or time of the COD decay (s in the case of CE), V_s is the solution volume (dm³), Δ COD is the COD reduction
125 (g dm⁻³) at time t , F is the Faraday constant (96487 C mol⁻¹) and the constant 8 is the oxygen equivalent mass
126 (q equiv⁻¹).

127 3 Results and Discussion

128 3.1 XRD analyses and SEM (and EDX)

129 To identify the crystal structure of the prepared electrodes XRD analysis was conducted. Fig. 1 shows XRD patterns
130 of the Ti/Ta₂O₅-SnO₂ electrodes annealed at 450, 550 and 650 °C. XRD pattern of the electrode annealed at 450 and
131 550 °C contained intense peaks of hexagonal Ti substrate appearing at $2\theta = 35.097, 38.269, 40.141, 52.898, 62.965,$
132 $70.444, 76.134$ and 77.348° associated to the (1 0 0), (0 0 2), (1 0 1), (1 0 2), (1 1 0), (1 0 3), (1 1 2) and (2 0 1)
133 crystal orientations of titanium, while XRD patterns of the electrode annealed at 650 °C showed the only clear peak
134 of hexagonal titanium at $2\theta = 40.141^\circ$. This could be explained by high crystallinity of Ta₂O₅ - SnO₂ films formed
135 at 650 °C. Tantalum was represented by orthorhombic β -Ta₂O₅ with peaks corresponding to the (0 0 1), (1 1 0), (2 0
136 0), (1 1 1), (2 0 1), (0 0 2), (3 1 0), (2 0 2), (3 1 2) and (4 0 2) planes and hexagonal δ -Ta₂O₅ with peaks
137 corresponding to (0 0 3), (2 0 0), (2 0 3), (0 0 6) and (2 2 0). Tetragonal cassiterite SnO₂ was evidenced through the
138 presence of (1 1 0), (1 0 1), (1 1 1), (2 1 1), (3 1 0), (3 0 1), (2 0 2), (3 2 1), (4 0 0) and (3 3 0) reflections. The
139 presence of tetragonal rutile TiO₂ in the Ti/Ta₂O₅-SnO₂ electrodes structure is explained by the oxygen solubility in
140 the metal lattice of the titanium substrate [25]. The main peaks of TiO₂ were corresponding to the (1 0 1), (2 0 0), (1
141 1 1), (2 1 0), (2 1 1), (2 2 0), (0 0 2), (3 1 0), (3 0 1) and (1 1 2) atomic planes. The low intensity of TiO₂, SnO₂ and
142 Ta₂O₅ peaks in the XRD pattern of the electrode annealed at 450 °C can be attributed to a low crystallinity of the
143 formed oxides and as a result to a low performance of this electrode towards MB oxidation (see below).

144 Fig. 2 shows typical SEM images and EDX element mapping of the Ti/Ta₂O₅-SnO₂ electrodes annealed at 450, 550
145 and 650 °C. In general, the SEMs show that the surfaces are very similar in appearance although the electrode
146 prepared at 550 °C does have more cavities and pin holes present which tends to suggest a potentially larger active
147 surface area for electrolysis. The surface roughness and porosity can influence diffusion to the electrode surface and
148 this is investigated in section 3.2. From the EDX mapping the Ta distribution (Fig. 2d – f) over Ti substrate is rather
149 scattered with the resulting Ta₂O₅ particles size varying from a few nanometers (dots on the mapping images) to a
150 few micrometers forming agglomerates (bright blue spots). Sn distribution over Ti substrate (Fig. 2g – i) is more or
151 less homogeneous with a greater accumulation on the electrode annealed at 550 °C and the smaller content on the
152 electrodes annealed at 450 °C and 650 °C.

153 3.2 Cyclic voltammetry

154 3.2.1 Characterization of electrodes

155 To estimate the relative electrode surface area after annealing, cyclic voltammograms were recorded from an
 156 electrolyte containing a simple redox couple, from electrodes prepared at the three chosen annealing temperatures.
 157 Figure 3 shows typical cyclic voltammograms recorded for a Ti/Ta₂O₅-SnO₂ electrode annealed at 550 °C from an
 158 aqueous solution of 0.5 mM K₄Fe(CN)₆ and 0.1 M Na₂SO₄ using a range of potential scan rates. The couple has the
 159 characteristics of a quasi-reversible electron transfer on this electrode surface; well-formed oxidation and coupled
 160 reduction peaks are observed around 0.25 V and 0.15 V respectively. The peak separations are greater than 60 mV
 161 expected for a reversible process (98 mV – 129 mV with the scan rates shown). However, this observation may
 162 simply be due to the high intrinsic resistance of this type of electrode material [26]. The value of the diffusion
 163 coefficient estimated from the slope of the linear I_p anodic against the square root of the sweep rate plot is 9.2·10⁻⁶
 164 cm² s⁻¹ which is in good agreement with literature reported values [27-30].

165 Peak currents were recorded from cyclic voltammograms run at slow scan rates. Table 1 shows the peak current
 166 densities and peak separations recorded at a sweep rate of 5 mV s⁻¹, for the oxidation of 0.5 mM K₄Fe(CN)₆ at three
 167 electrode annealing temperatures and for comparison an entry for a gold disc electrode is also included.

168 **Table 1.** Peak currents for the oxidation of 0.5 mM K₄Fe(CN)₆ in 0.1 M Na₂SO₄ for Ti/Ta₂O₅-SnO₂ electrodes and a
 169 Au electrode recorded at a scan rate of 5 mV s⁻¹

Electrode	Annealing temperature, °C	Peak Current Density, μA cm ⁻²
	450	41.2
Ti/Ta ₂ O ₅ -SnO ₂	550	35.4
	650	32.8
Au disc electrode	-	22.1

170

171 In general, the peak current densities observed at the Ti/Ta₂O₅-SnO₂ electrodes are of the same order of magnitude
 172 with the lowest value recorded for the highest firing temperature. However, the recorded currents are all higher than
 173 that recorded from the smooth gold electrode. This observation suggests that Ti/Ta₂O₅-SnO₂ electrodes prepared
 174 using the thermal decomposition technique described in [22] and imaged in Figure 2, lead to rough electrode

175 surfaces with approximately twice the active working area available. It is unclear why the peak currents are reduced
176 at the higher firing temperature of 650 °C. Other workers have observed similar effects with different oxide
177 electrodes and have suggested that the formation of a poorly conducting oxide layer between the Ta₂O₅-SnO₂
178 coating and the metal substrate interferes with the electron transfer process [31]. It was found that electrical
179 conductivity of Sn_{0.97}Ta_{0.03}O₂ thin films grown on TiO₂ substrates and annealed at 500 – 600 °C is approximately
180 1100 S m⁻¹ [32]. Trasatti suggests that lower crystallinity may be important. However from the XRD data, see
181 above, a reduced degree of crystallinity was only recorded at 450 °C and the electron transfer for the ferricyanide
182 redox couple proceeds rapidly at this surface.

183 3.2.2 MB Oxidation

184 Fig. 4a shows the CV results of prepared Ti/Ta₂O₅-SnO₂ electrodes recorded from a working solution of 0.1 mM
185 MB and 0.1 M Na₂SO₄. All voltammograms, with the exception of electrode annealed at 450 °C contained an anodic
186 current peak with a maximum at potential of 1.1 V absent on CVs in the blank solution and attributed to oxidation of
187 MB [22]. Anodic current of 60 μA cm⁻² at potential of 1.1 V is 3 and 8 times higher for the electrode annealed at
188 550 °C than for electrodes annealed at 650 °C and 450 °C respectively. The higher capacitance current observed
189 from the electrode annealed at 550 °C also confirms a greater microroughness. Therefore, at an annealing
190 temperature of 550 °C the tantalum/tin oxide coating shows some promise as a non-precious metal electrode for the
191 electrocatalytic oxidation of MB. Further investigations at different pHs were carried out to determine the optimum
192 conditions for MB oxidation.

193 To investigate the electrochemical behavior of prepared Ti/Ta₂O₅-SnO₂ electrodes in different media CVs were run
194 in the working solutions of 0.1 M Na₂SO₄ and MB at pH 2, 6.5 and 12. Figure 4b represents the CV results in 0.1 M
195 Na₂SO₄ and 0.1 mM MB aqueous solution at the pH 2, 6.5 and 12. Voltammograms recorded at pH 6.5 and at pH =
196 2 showed anodic current peaks of 60 and 30 μA cm⁻² respectively attributed to the MB oxidation. However, when
197 pH was changed to the value of 12, no anodic current of MB oxidation was observed (Inset Fig. 4b). The absence of
198 MB oxidation peak is explained by a significant shift of the OER onset potential to more negative values from about
199 1.8 V to 1.4 V and masks the MB oxidation peak. Running an electrolysis process in alkali is therefore more
200 favorable for oxygen formation rather than MB oxidation.

201 To ensure an efficient electrolysis process the concentration of the electroactive species near the surface of the
202 electrode should be maintained and not depleted. Typically, this is achieved on an industrial scale by efficient
203 agitation of the electrolyte using a number of techniques for example rapid stirring, pumping or using turbulence
204 promoters [33]. Ultrasound can also be used to improve mass transport. The advantages of applying ultrasonic
205 irradiation are twofold: firstly it can increase the movement of electroactive species to the electrode surface and
206 secondly through the process of cavitation hydroxyl radicals can be generated and thereby increase the rate of
207 oxidation of MB.

208 Figure 5 records the first and sixth cyclic voltammograms from an electrochemical cell without agitation (5a), using
209 a magnetic stirrer (5b) and with a 30 kHz ultrasonic field applied (5c). The cyclic voltammogram without agitation
210 shows the characteristic depletion of the electroactive species and gradually decreases with time whereas stirred and
211 ultrasonically irradiated cells show no change in the current response. The MB is replenished as fast as it is
212 consumed at the electrode surface. Applying ultrasound to any laboratory cell will therefore ensure good electrolyte
213 movement and through cavitation generate radicals which have the potential to accelerate the oxidation of MB.

214 *3.3 Electrolysis (Degradation experiments)*

215 To prove electrocatalytic activity of Ti/Ta₂O₅-SnO₂ electrodes towards MB oxidation and show the effect of
216 different media on MB degradation rates a series of electrolysis experiments was conducted with 0.1 mM MB and
217 0.1 M Na₂SO₄ solution using magnetic stirring. Preparative electrolysis tests in an ultrasonic field are reported in
218 [34]. According to Fig. 6a 95% and 85% decolourisation efficiency was achieved in two hours of electrolysis at pH
219 of 6.5 and 2 respectively. Degradation rate of MB in basic media was considerably slower and reached only 78%
220 after 2 h of electrochemical oxidation that coincides with the preliminary prediction obtained by CV measurements
221 (Fig. 4b) and was attributed to a low oxygen evolution overvoltage [35-36]. Efficiency of Ti/Ta₂O₅-SnO₂ electrodes
222 in regards of MB oxidation was confirmed by the data on COD and NPOC removal (Fig. 6b, inset Fig. 6a). The
223 fastest COD removal efficiency was obtained at a pH of 6.5 and after 2 h of electrolysis was equal to 85%. It
224 increased slowly to 90% and was stable during 8 h of electrochemical oxidation. Lower COD removal values were
225 achieved after 2h of electrolysis at pH of 2 (70%) and 12 (26%). However, COD removal efficiency increased to 85
226 – 99% for all media after 8 h of electrolysis. Mineralization data obtained during electrolysis showed that MB was

227 mostly oxidized to CO₂. Overall NPOC reduction (Inset Fig. 6a) of 71, 74 and 76% was reached after 8 h of
 228 electrolysis for the electrodes annealed at 550 °C at pH of 12, 6.5 and 2 respectively.

229 Table 2 shows the data on EC required for the complete decolourisation and 80% COD decrease of 0.1 mM MB and
 230 0.1 M Na₂SO₄ solution and CE obtained at 80% COD reduction in different media of working solution. Electrolyses
 231 in acidic media was the most energy effective for conducting decolourisation experiments and required 7.7 kWh m⁻³
 232 of energy to achieve 100% colour removal. Basic and original media of working solution needed 24.4 and 21.5 kWh
 233 m⁻³ respectively to obtain 100% decolourisation. The EC data are comparable to those required for decolourisation
 234 of other organic dyes [37-39]. The original media of working solution was the most energy effective towards COD
 235 reduction and basic media was the least effective. The energy required for 80% COD decrease at pH = 6.5 was equal
 236 to 9.3 kWh m⁻³ versus 33.9 kWh m⁻³ consumed at pH = 12. The highest CE of 10.1% was observed for the lowest
 237 EC of 9.3 kWh m⁻³ required for 80% COD removal at pH = 6.5 that is a typical behavior for many mixed metal
 238 oxide electrodes [40-42]. The lowest CE of 1% was obtained for 80% COD decrease in basic conditions which was
 239 attributed to oxygen evolution being the favored reaction.

240 **Table 2** EC (kWh m⁻³) and CE (%) obtained at complete decolourisation and 80% COD reduction of 0.1 mM MB in
 241 0.1 M Na₂SO₄ solution at pH of 6.5, 2 and 12 for the electrodes annealed at 550 °C and at pH of 6.5 for the electrode
 242 annealed at 650 °C

Electrode annealing temperature and electrolysis media	EC (kWh m ⁻³) at 100% decolourisation	EC (kWh m ⁻³) at 80% COD reduction	CE (%) at 80% COD reduction
550 °C, pH = 2	7.7	12.9	5.2
550 °C, pH = 6.5	21.5	9.3	10.1
550 °C, pH = 12	24.4	33.9	1

243

244 4 Conclusion

245 The annealing temperature of Ti/Ta₂O₅-SnO₂ electrodes and working media for electrocatalytic oxidation of MB
 246 was investigated. The electrodes were characterized by XRD, SEM and EDX analysis. Cyclic voltammetry
 247 suggested the electrode surface area of Ti/Ta₂O₅-SnO₂ electrodes annealed at 550 °C was high in comparison with

248 an electroplated Pt electrode. An annealing temperature of 550 °C showed the best electrocatalytic activity for
249 oxidation of MB. The original media of the 0.1 M Na₂SO₄ and 0.1 mM MB solutions was found optimal for
250 conducting degradation experiments since it gave high anodic currents of OER and provided decolourisation, COD
251 and TOC removal efficiencies analogous to that in acidic media. Moreover, this media was the most energy effective
252 towards COD decrease providing the lowest value of EC and highest value of CE. Acidic conditions were found
253 energy effective for achieving complete color removal. Decrease of Ti/Ta₂O₅-SnO₂ electrodes efficiency toward MB
254 decolourisation and COD removal during the electrocatalytic oxidation at pH = 12 was observed due to a low OER
255 overvoltage and current leakage for water oxidation. Ultrasonic field showed the improved electrodes performance
256 towards MB oxidation due to enhancement of MB mass transport to the electrode surface which was supported by
257 the data on diffusion controlled process.

258 **Acknowledgments**

259 This work was supported by Maj and Tor Nessling Foundation.

260

261 **References**

262

- [1] M. Beck, R. Vallarroel Walker (2013) On water security, sustainability, and the water-food-energy-climate nexus. *Front. Environ. Sci. Eng.* 7:626 – 639
- [2] M. El-Shahawi, A. Hamza, A. Bashammakh, W. Al-Saggaf (2010) An overview on the accumulation, distribution, transformations, toxicity and analytical methods for the monitoring of persistent organic pollutants, *Talanta* 80:1587 – 1597
- [3] U. Pagga, D. Brown (1986) The degradation of dyestuff: Part II behaviour of dyestuff in aerobic biodegradation tests. *Chemosphere* 15:479 – 491.

- [4] C. Comninellis (1994) Electrocatalysis in the electrochemical conversion/combustion of organic pollutants for wastewater treatment. *Electrochim. Acta* 39:1857 – 1862
- [5] J. Fan, G. Zhao, H. Zhao, S. Chai, T. Cao (2013) Fabrication and application of mesoporous Sb-doped SnO₂ electrode with high specific surface in electrochemical degradation of ketoprofen. *Electrochim. Acta* 94:21 – 29.
- [6] R. E. Palma-Goyes, J. Silva-Agreto, I. González, R. A. Torres-Palma (2014) Comparative degradation of indigo carmine by electrochemical oxidation and advanced oxidation processes. *Electrochim. Acta* 140:427 - 433
- [7] A. El-Ghenemy, F. Centellas, J. A. Garrido, R. M. Rodríguez, I. Sirés, P. L. Cabot, E. Brillas (2014) Decolorization and mineralization of Orange G azo dye solutions by anodic oxidation with a boron-doped diamond anode in divided and undivided tank reactors. *Electrochim. Acta* 130:568 -576
- [8] J. M. Aquino, R. Rocha-Filho, L. Ruotolo, N. Bocchi, S. Biaggio (2014) Electrochemical degradation of a real textile wastewater using b-PbO₂ and DSA® anodes. *Chem. Eng. J.* 251:138 - 145
- [9] D. Shao, J. Liang, X. Cui, H. Xu, W. Yan (2014) Electrochemical oxidation of lignin by two typical electrodes: Ti/Sb-SnO₂ and Ti/PbO₂. *Chem. Eng. J.* 244:288–295
- [10] L. Da Silva, D. Franco, L. De Faria, J. Boodts (2004) Surface, kinetics and electrocatalytic properties of Ti/(IrO₂+ Ta₂O₅) electrodes, prepared using controlled cooling rate, for ozone production. *Electrochim. Acta* 49:3977–3988
- [11] L. Xu, Y. Xin, J. Wang (2009) A comparative study on IrO₂-Ta₂O₅ coated titanium electrodes prepared with different methods. *Electrochim. Acta* 54:1820–1825
- [12] J. Kong, S. Shi, X. Zhu, J. Ni (2007) Effect of Sb dopant amount on the structure and electrocatalytic capability of Ti/Sb-SnO₂ electrodes in the oxidation of 4-chlorophenol. *J. Environ. Sci.* 19:1380–1386
- [13] B. Adams, M. Tian, A. Chen (2009) Design and electrochemical study of SnO₂-based mixed oxide electrodes.

Electrochim. Acta 54:1491–1498

- [14] L. Yue, L. Wang, F. Shi, J. Guo, J. Yang, J. Lian, X. Luo (2015) Application of response surface methodology to the decolorization by the electrochemical process using $\text{FePMo}_{12}\text{O}_{40}$ catalyst. *J. Ind. Eng. Chem.* 21:971 - 979
- [15] M. Zhou, H. Särkkä, M. Sillanpää (2011) A comparative experimental study on methyl orange degradation by electrochemical oxidation on BDD and MMO electrodes. *Sep. Purif. Technol.* 78:290–297
- [16] L. García-Cruz, A. Sáez, C. O. Ania, J. Solla-Gullón, T. Thiemann, J. Iniesta, V. Montiel (2014) Electrocatalytic activity of Ni-doped nanoporous carbons in the electrooxidation of propargyl alcohol. *Carbon* 73:291 – 302
- [17] T. Gan, C. Hu, Z. Chen, S. Hu (2011) Novel electrocatalytic system for the oxidation of methyl jasmonate based on layer-by-layer assembling of montmorillonite and phosphotungstic acid nano hybrid on graphite electrode. *Electrochim. Acta.* 56:4512–4517
- [18] Y. Zhao, C. Li, W. Zhao, Q. Du, B. Chi, J. Sun, Z. Chai, X. Wang (2013) Electrocatalytic oxidation of ascorbic acid on a lithium-doped tantalum oxide film coated electrode. *Electrochim. Acta* 107:52– 58
- [19] Y. Wang, Q. Liu, Q. Qi, J. Ding, X. Gao, Y. Zhang, Y. Sun (2013) Electrocatalytic oxidation and detection of N-acetylcysteine based on magnetite/reduced graphene oxide composite-modified glassy carbon electrode. *Electrochim. Acta* 111:31– 40
- [20] A. Ghoniem, B. . El-Anadouli, M. Saleh (2013) Electrocatalytic glucose oxidation on electrochemically oxidized glassy carbon modified with nickel oxide nanoparticles. *Electrochim. Acta* 114:713– 719
- [21] J. Kim, J. Lee, Y. Tak (2009) Relationship between carbon corrosion and positive electrode potential in a proton-exchange membrane fuel cell during start/stop operation. *J. Power Sources* 192:674–678
- [22] M. Shestakova, P. Bonete, R. Gómez, M. Sillanpää, W. Z. Tang (2014) Novel $\text{Ti-Ta}_2\text{O}_5\text{-SnO}_2$ electrodes for

water electrolysis and electrocatalytic oxidation of organics. *Electrochim. Acta* 120:302 – 307

- [23] C. Comninellis, G. Vercesi (1991) Problems in DSA® coating deposition by thermal decomposition. *J. Appl. Electrochem.* 21:136–142
- [24] C. Martínez-Hutile, E. Brillas (2009) Decontamination of wastewaters containing synthetic organic dyes by electrochemical methods: A general review. *Appl. Catal. B-Environ.* 87:105 – 145
- [25] N. Greenwood, A. Earnshaw (1997) *Chemistry of the Elements*, 2nd ed., Butterworth-Heinemann, Elsevier, Oxford
- [26] M. M. Barsan, E. M. Pinto, M. Florescu, C. M. A. Brett (2009) Development and characterization of a new carbon composite electrode. *Anal. Chim. Acta* 635:71 – 78
- [27] B. K. Gu, Y. A. Ismail, G. M. Spinks, S. I. Kim, I. So, S. J. Kim (2009) A linear actuation of polymeric nanofibrous bundle for artificial muscles. *Chem. Mater.* 21:511 – 515
- [28] E. P. Rivero, F. F. Rivera, M. R. Cruz-Díaz, E. Mayen, I. González (2012) Numerical simulation of mass transport in a filter press type electrochemical reactor FM01-LC: Comparison of predicted and experimental mass transfer coefficient. *Chem. Eng. Res. Des.* 90:1969-1978
- [29] Z. O. Ameer, M. M. Husein (2013) Electrochemical Behavior of Potassium Ferricyanide in Aqueous and (w/o) Microemulsion Systems in the Presence of Dispersed Nickel Nanoparticles. *Sep. Sci. Technol.* 48:681–689
- [30] S. Menolasina (2005) Electrochemical studies of $\text{Fe}(\text{CN})_{64-}/\text{Fe}(\text{CN})_{63-}$ on gold ultramicroelectrodes varying the concentrations of KF as supporting electrolyte. *Rev. Téc. Ing. Univ. Zulia* 28:159 – 168
- [31] S. Trasatti (1987) Oxide/aqueous solution interfaces, interplay of surface chemistry and electrocatalysis. *Mater. Chem. Phys.* 16:157 – 174
- [32] H. Toyosaki, M. Kawasaki, Y. Tokura (2008) Electrical properties of Ta-doped SnO_2 thin films epitaxially grown on TiO_2 substrate. *Appl. Phys. Lett.* 93:132109-1-132109-3.

- [33] D. Pletcher, F. Walsh (1990) *Industrial Electrochemistry*, Springer Science & Business Media
- [34] M. Shestakova, M. Vinatoru, T. J. Mason, M. Sillanpää (2015) Sonoelectrocatalytic decomposition of methylene blue using Ti/Ta₂O₅-SnO₂ electrodes. *Ultrason. Sonochem.* 23:135 – 141
- [35] R. Kötz, S. Stucki, B. Carcer (1991) Electrochemical waste water treatment using high overvoltage anodes. Part I: Physical and electrochemical properties of SnO₂ anodes. *J. Appl. Electrochem.* 21:14 – 20.
- [36] S. Stucki, R. Kötz, B. Carcer, W. Suter (1991) Electrochemical waste water treatment using high overvoltage anodes. Part II: Anode performance and applications. *J. Appl. Electrochem.* 21:99 - 104
- [37] L. Andrade, L. Ruotolo, R. Rocha-Filho, N. Bocchi, S. Biaggio, J. Iniesta, V. García-García, V. Montiel (2007) On the performance of Fe and Fe,F doped Ti-Pt/PbO₂ electrodes in the electrooxidation of the Blue Reactive 19 dye in simulated textile wastewater. *Chemosphere* 66:2035-2043
- [38] C. Cameselle, M. Pazos, M. Sanromán (2005) Selection of an electrolyte to enhance the electrochemical decolourisation of indigo. Optimisation and scale-up. *Chemosphere* 60:1080 – 1086
- [39] V. López-Grimau, M. Gutiérrez (2006) Decolourisation of simulated reactive dyebath effluents by electrochemical oxidation assisted by UV light. *Chemosphere* 62:106 – 112
- [40] L. Andrade, R. Rocha-Filho, N. Bocchi, S. Biaggio, J. Iniesta, V. García-García, V. Montiel (2008) Degradation of phenol using Co- and Co, F-doped PbO₂ anodes in electrochemical filter-press cells. *J. Hazard. Mater.* 153: 252 – 260
- [41] D. Rajkumar, J. Kim, K. Palanivelu (2005) Indirect electrochemical oxidation of phenol in the presence of chloride for wastewater treatment. *Chem. Eng. Technol.* 28:98 – 105
- [42] Y. Yavuz, A. Koparal (2006) Electrochemical oxidation of phenol in a parallel plate reactor using ruthenium mixed metal oxide electrode. *J. Hazard. Mater.* 136:296 – 302

263

264 **Figure captures**

265 **Fig. 1** X-Ray diffractograms for Ti/Ta₂O₅-SnO₂ electrodes annealed at 450, 550 and 650 °C

266 **Fig. 2** SEM images of Ti/Ta₂O₅-SnO₂ electrodes with element-mapping: (d – f) Ta mapping, (g – i) Sn mapping and
267 for the electrodes annealed at (a) 550, (b) 650 and (c) 450 °C respectively

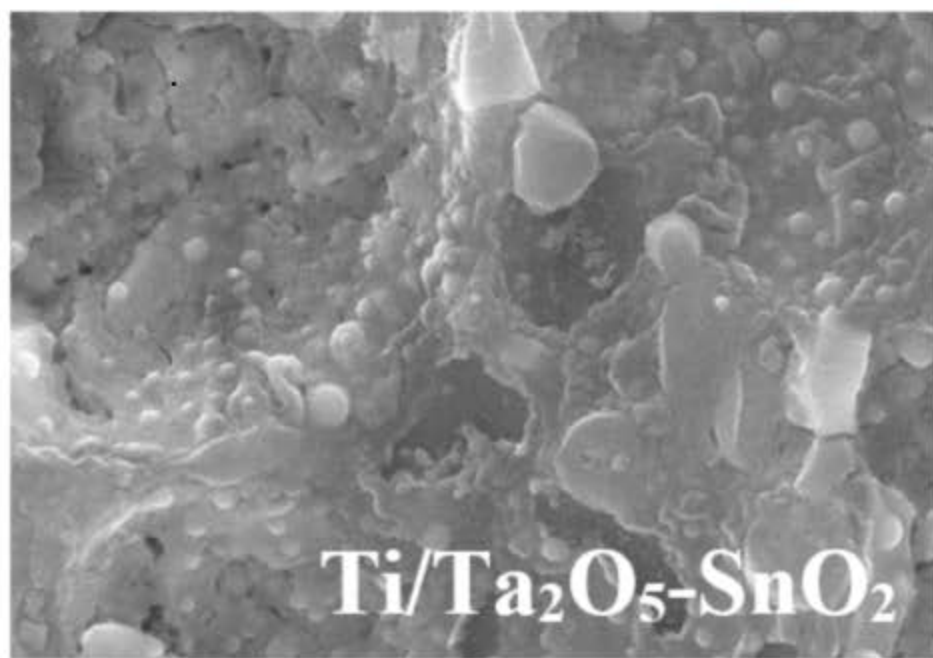
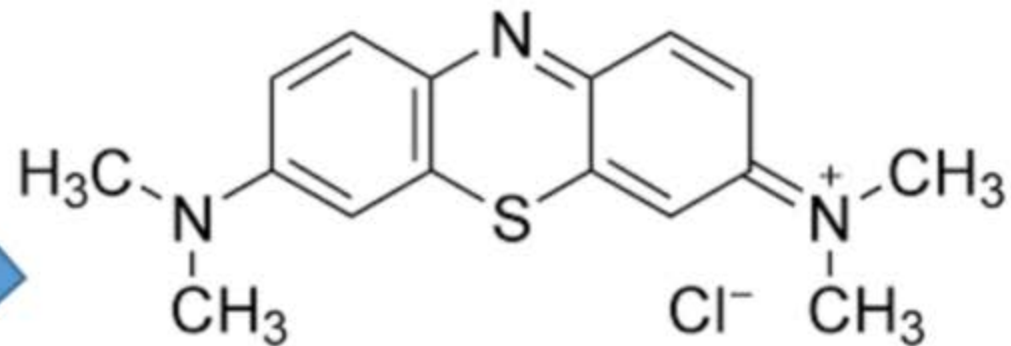
268 **Fig. 3** CVs Ti/Ta₂O₅-SnO₂ electrode annealed at 550 °C in 0.5 mM K₄Fe(CN)₆·3H₂O and 0.1 M Na₂SO₄ at different
269 scan rates ν

270 **Fig. 4** CV of Ti/Ta₂O₅-SnO₂ electrodes prepared at different temperatures (Fig. 4a) and run in different media (Fig.
271 4b) in working solution of 0.1 mM MB and 0.1 M Na₂SO₄ (Fig 4b) adjusted to of pH = 2 and pH = 12 (Inset Fig.
272 4b) with H₂SO₄ or NaOH respectively for Ti/Ta₂O₅-SnO₂ electrode annealed at 550 °C. $\nu = 50 \text{ mV s}^{-1}$

273 **Fig. 5** Different CV scans made in the working solution of 0.1 mM MB and 0.1 M Na₂SO₄ in acidic media (pH = 2)
274 without external exposure (Fig. 5a), under the influence of ultrasonic field (Fig. 5b) and with magnetic stirrer (Fig.
275 5c). $\nu = 50 \text{ mV s}^{-1}$

276 **Fig. 6** Colour (a) and COD (b) removal efficiency after 8h of electrolysis of 0.1 M Na₂SO₄ and 0.1 mM MB
277 working solution. Inset Fig. 6a: NPOC removal efficiency (mineralization)

278



+ 9 mA cm⁻²

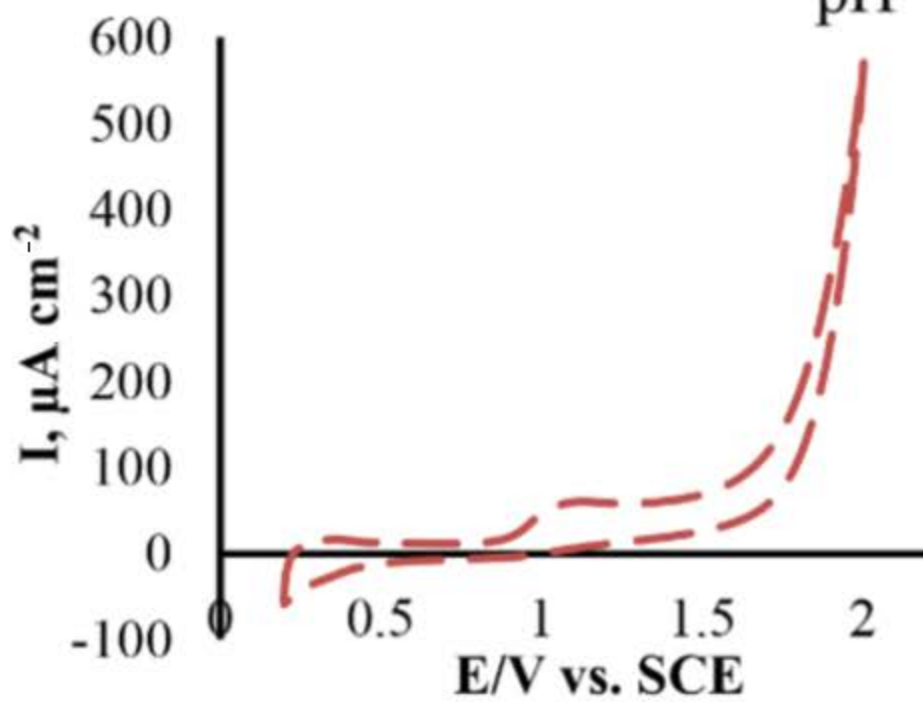
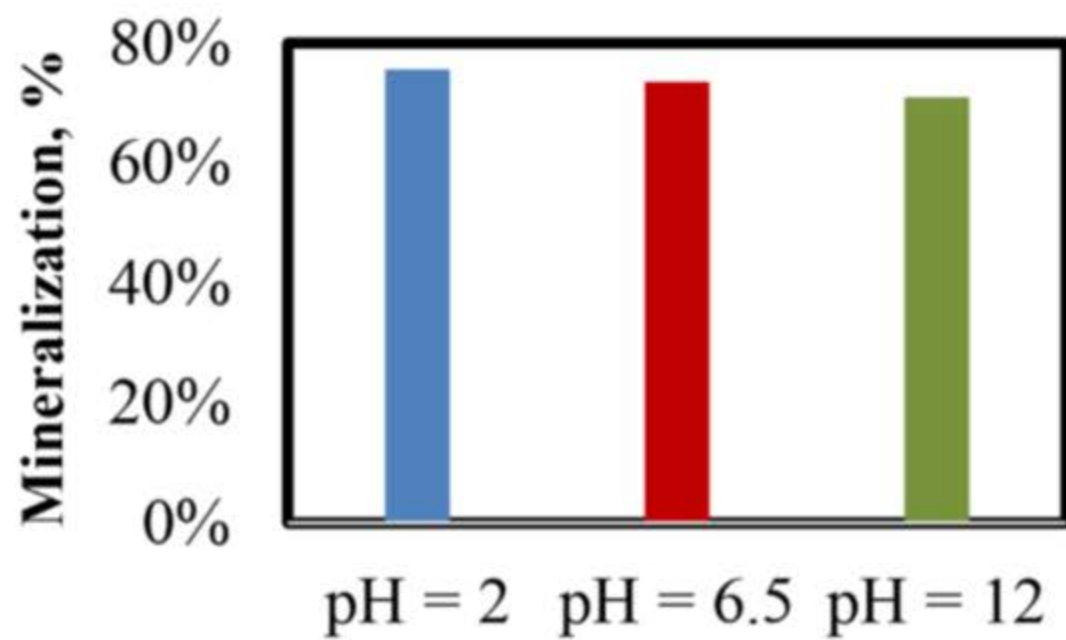
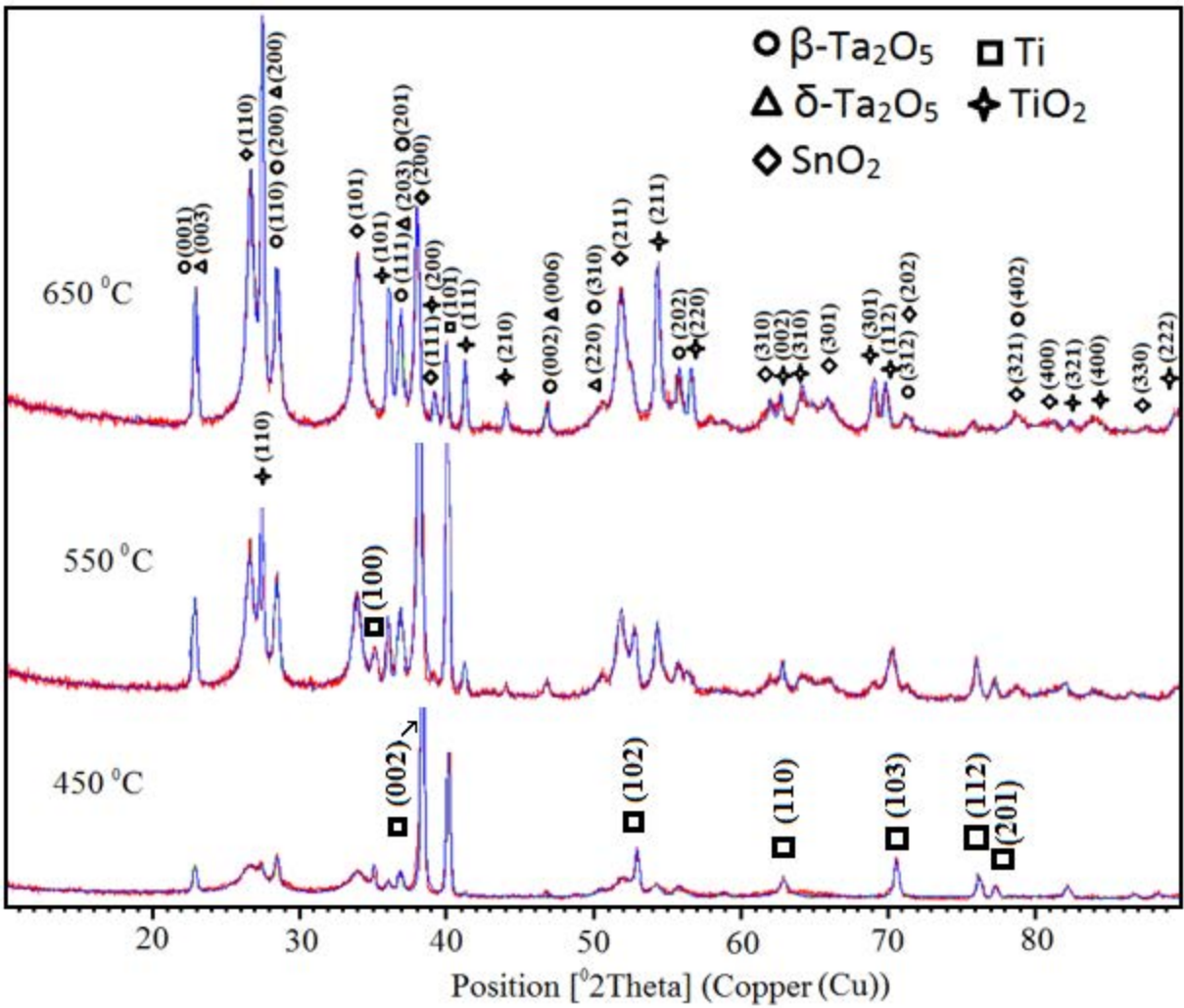


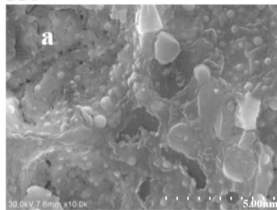
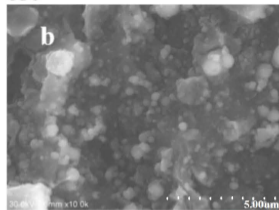
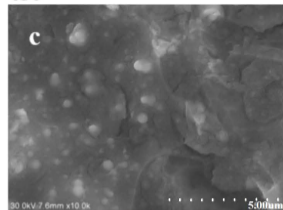
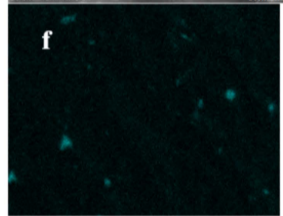
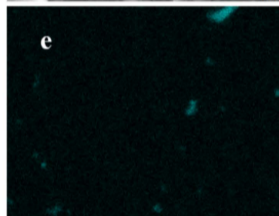
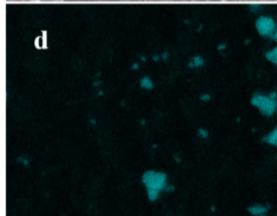
Table 1. Peak currents for the oxidation of 0.5 mM $K_4Fe(CN)_6$ in 0.1 M Na_2SO_4 for Ti/Ta₂O₅-SnO₂ electrodes and a Au electrode recorded at a scan rate of 5 mV s⁻¹

Electrode	Annealing temperature, °C	Peak Current Density, μA cm ⁻²
	450	41.2
Ti/Ta ₂ O ₅ -SnO ₂	550	35.4
	650	32.8
Au disc electrode	-	22.1

Table 2. EC (kWh m⁻³) and CE (%) obtained at complete decolourisation and 80% COD reduction of 0.1 mM MB in 0.1 M Na₂SO₄ solution at pH of 6.5, 2 and 12 for the electrodes annealed at 550 °C and at pH of 6.5 for the electrode annealed at 650 °C

Electrode annealing temperature and electrolysis media	EC (kWh m ⁻³) at 100% decolourisation	EC (kWh m ⁻³) at 80% COD reduction	CE (%) at 80% COD reduction
550 °C, pH = 2	7.7	12.9	5.2
550 °C, pH = 6.5	21.5	9.3	10.1
550 °C, pH = 12	24.4	33.9	1



550**650****450****Ta****Sn**